A Search for Radiative Rare B Decays with the DELPHI Detector at LEP

M. Battaglia[1] and D. Liko[2]

Abstract

The decay b $\rightarrow$ sγ is forbidden at the tree level and occurs through radiative FCNC loop diagrams. The inclusive rate of this process is sensitive to the top quark mass, its couplings and to new physics beyond the Standard Model. A search for the exclusive decays B $\rightarrow$ K$^*\gamma$ was performed using the statistics collected with the DELPHI detector at the LEP collider during 1991 and 1992. Several of the higher K* resonances were investigated. A particular benefit derived from the particle identification and tracking resolution capabilities of the DELPHI detector allowing to reduce the background sources. The combined use of Ring Imaging Cherenkov detector and specific ionization in the TPC provided a pure sample of K mesons with high efficiency thus reducing the combinatorial background. The information from a high resolution silicon microvertex detector permitted to reject contribution from light quark decays of the Z^0. Preliminary results are presented. In addition also preliminary results from a search for non radiative decays, B $\rightarrow$ Kπ(K) are shown.

[1]SEFT, Helsinki
[2]HEPHY,Vienna

1 Introduction

The number of events collected by the DELPHI detector at LEP has reached about one million hadronic decays of the Z^0 Boson. Using that statistic already a considerable number of exclusive decays of B Hadrons are accesable. The number of exclusive decays, that can be reconstructed, is given by

$$Nr.\ of\ Z^0 \times 2 \times \frac{\Gamma_{b\bar{b}}}{\Gamma_{\rm had}} \times f_{\rm B} \times \epsilon_{\rm B}, \tag{1}$$

where $f_{\rm B}$ is the branching ratio and $\epsilon_{\rm B}$ the reconstruction efficiency for a given decay channel. The study of exclusive decays of B Hadrons is profitting from the detector capabilities, which allow topological tagging of b decays and efficient particle identification.

The current sensitivity given by that statistic allows to study decays with branching ratios of the order of 10^{-3}–10^{-4}. Therefore a large spectrum of exclusive decay modes is already under study and more will be in reach in the near future. The search for rare decays of B Hadrons, which are at the sensitivity threshold, is of special interest.

In this analysis preliminary results from a search of radiative rare B decays involving flavor changing neutral currents are presented. The standard model prediction, including QCD corrections, for the branching ratio $BR(\mathrm{b} \to \mathrm{s}\gamma)$ is of the order of $2 - 5{\times}10^{-4}$. About 40 to 90% of the decays are accesable through exclusive channels. The search has been performed in the channels $B^{(0,-)} \to K^*\gamma$ and $B_s \to \phi\gamma$.

In addition preliminary results of a search for non radiative decays $b \to sq\bar{q}$ has been performed. The expected branching ratio for these decays is of the order of 10^{-3}, where rates of about 1% are expected in various exclusive channels. The channels studied were $B^0 \to K\pi$ and $B_s \to KK$.

2 The analysis procedure

For the analysis the data collected during the years 1991 and 1992 were used. In total 947K hadronic events were accepted by the hadronic event selection. About half of the data contain information from the DELPHI Ring Imaging Cherenkov detector (BRICH).

The search for radiative decays was performed in the channels

- $B^0 \to K^*(892)^0\gamma$, $K^*(892)^0 \to K^+\pi^-$
- $B^0 \to K_2^*(1430)^0\gamma$, $K_2^*(1430)^0 \to K^+\pi^-$
- $B^- \to K_1(1270)^-\gamma$, $K_1(1270)^- \to K^-\rho^0$
- $B_s \to \phi(1020)\gamma$, $\phi(1020) \to K^+K^-$

As all final states involve at least one Kaon and a photon, efficient particle identification and photon reconstruction is essential for the analysis.

2.1 Particle identification

Kaon were identified using the specific energy loss in the TPC and the BRICH. Photons were reconstructed using the electromagnetic calorimeter. The vertex detector was used to suppress background from light quark events by requiring a positive flight distance.

The information on the specific energy loss (dE/dx) in the TPC is provided by up to 192 sampling points. The obtained resolution is about 7%. In the region of relativistic rise, above 3 – 4 GeV, a Kaon - Pion separation of 1.5 σ is reached (see figure 1).

In the Cherenkov Ring Imaging detector Kaon identification is achieved over a large momentum range by the combined use of two radiators:

- a liquid radiator with a single photo electron resolution of 12 mrad in the low momentum region, and
- a gas radiator with a single photo electron resolution of 4.5 mrad in the high momentum region.

In this analysis only the gas radiator was used (see figure 2). In the momentum range between 3.5 and 9 GeV/c Kaons produce no light and can be separated from the light particles, which are still above the threshold ('veto identification'). In the higher momentum region, between 9 and 20 GeV/c, Kaon identification is based on measurement of the Cherenkov angle ('ring identification').

The particle trajectories are reconstructed with high precision by the combined DELPHI tracking system including the silicon vertex detector (VD). The measured extrapolation accuracy to the interaction region in hadronic events is $\sqrt{69^2/p_t^2 + 24^2}$ μm. For high momentum tracks in $Z^0 \to \mu^+\mu^-$ events a resolution of 26 μm is reached (see figure 3). Secondary vertex reconstruction separates heavy flavor decay products from hadronisation particles.

The High Density Projection Chamber (HPC) in the barrel region is a gas sampling calorimeter providing three-dimensional charge distribution measurements with high granularity. The 40 layers of lead radiator have 17 interaction length. Figure 4 shows the obtained energy resolution, measured with Bhabhas events in the high momentum region and Compton events in the low momentum region. The forward region is covered by a lead glass calorimeter, the FEMC.

2.2 Particle reconstruction

Identified Kaons, with a momentum above 4 GeV/c, were combined with any opposite charge particle in the same jet with momentum above 2 GeV/c. The secondary vertex was reconstructed and vertices with an χ^2-probability less than 0.001 were rejected. For the K* candidates an energy, E_{K^*}, above 10 GeV and a positive flight distance, $d/\sigma_d > 0$, was required. In figure 7 the obtained $K\pi$ invariant mass spectrum is shown. The final K* candidates were then selected in an interval around the expected mass $|m_{\mathrm{K}\pi} - m^*_{\mathrm{K}}| < 1.5\sigma_{\mathrm{K}^*}$.

A similar procedure was used to reconstruct ϕ candidates. To achive a high efficiency, only one tagged Kaon was required. As the opening angle of the decay $\phi \to$ KK is very small, less than 8 mrad, the reconstructed decay distance is less precise. ϕ candidates were therefore selected by requiring a small opening angle and reconstructed vertex within 3 cm of the interaction region.

Photons were reconstructed from electromagnetic showers in the HPC and the FEMC. In the HPC it was required that the shower starting point was before the forth layer and that energy was deposited at least in two consecutive layers. Showers associated to charged tracks were rejected. An energy $E_\gamma > 5$ GeV was required. In addition it was demanded that the angle between the reconstructed shower direction and the photon direction was compatible ($\Delta\theta < 0.1$ rad and $\Delta\phi < 0.1$ rad), to remove badly reconstructed showers.

As independent crosscheck for the massreconstruction using electromagnetic showers, decays K$^*(892)^- \to$ K$^-\pi^0$, produced in Z$^0 \to \tau^+\tau^-$ events, were studied. The decay products have a momentum range similar to decay products of the B Hadrons in the studied rare decays. Figure 6 shows an example for the invariant mass reconstruction using electromagnetic clusters, comparing data and Monte Carlo simulation. A good agreement was observed.

Finally B candidates were reconstructed. An energy $E_{\mathrm{B}} > 25$ GeV was required. The angle between the photon and the K* had to be smaller than 35°. Background events were suppressed by selecting events with less than 4 particles with a momentum $p > 3$ GeV/c. It was required that the candidate had an invariant mass, m_{B}, between 4.9 and 5.6 GeV/c^2. For candidates with photons reconstructed close to the edges of the HPC, where showers may not be fully contained, the interval was increased to 4.6 to 5.6 GeV/c^2 (see figure 5).

2.3 Efficiency and background studies

Simulated events generated with JETSET 7.3 PS and the full detector simulation have been used.

To study the reconstruction efficiency a dedicated production of several thousand decays for channel had been studied. A typical efficiency of 5 to 9% has been found.

To study the background 1600 K simulated hadronic events were used. It was found that the main background is due to $s\bar{s}$ and $c\bar{c}$ events. In addition photons were faked by energetic π^0 and η particles, which were not resolved in the electromagnetic calorimeter.

Table 1: Summary of results for the search for radiative decays. The quoted upper limit derived by CLEO for the channel $B^0 \to K^*(892)^0\gamma$ is based on their observation of the decay.

Channel	Nr. of Events	$BR \times 10^{-4}$	
		DELPHI Preliminary	Published Results
$B^0 \to K^*(892)^0\gamma$	< 3.4	< 3.6	< 0.75 (CLEO 93)[1]
$B^- \to K_1(1270)^-\gamma$	< 3.5	< 21	< 66 (ARGUS 89)[2]
$B^0 \to K_2^*(1430)^0\gamma$	< 8.1	< 18	< 4.4 (ARGUS 89)[2]
$B_s \to \phi(1020)\gamma$	< 3.4	< 19	

Particle identification efficiencies and misidentification ratios had been fixed to constant values. To evaluate the branching ratio the particle misidentification rates and efficiencies were measured from the data and applied to the simulation by a weighting technique. The obtained invariant mass distribution in the simulation was normalized to the data according to the relative number of events. A very good agreement between data and Monte Carlo simulation was observed.

3 Results

For the different decay channels the number of events within the considered mass interval was compared between data and Monte Carlo simulation. Using Poissonian statistic an upper limit for the number of observed signal events with a confidence level of 90% was derived.

The number of events observed in the data was very small, of the order of 0 to 6. As the Monte Carlo events were derived from a higher statistic, they had been reweighted and a more precise estimation of the expected background events was derived. Additional events observed in the data could significantly change the limit. To be conservative the mass interval was shifted of the order of ± 100 MeV and the interval which provided the maximum number of entries was selected.

Table 2: Summary of results for the search for non radiative decays.

Channel	Nr. of Events	$BR \times 10^{-4}$	
		DELPHI Preliminary	Published Results
$B^0 \rightarrow K\pi$	< 3.8	< 1.5	< 0.9 (CLEO 89)[3]
$B^0 \rightarrow KK$			

The invariant mass spectrum for the different channels is shown in figure 8 to 11.

The limits obtained include statistical errors only. Preliminary results from the search for radiative rare decays are summarized in table 1.

The search for non radiative rare decays was performed in the channels

- $\mathrm{B_d^0} \rightarrow \mathrm{K}\pi$, and
- $\mathrm{B_s^0} \rightarrow \mathrm{KK}$

In the analysis events were selected by requiring only one identified Kaon to obtain optimal efficiency. As consequence Kπ and KK final states were not separated and an inclusive limit for $B^0_{(\mathrm{d,s})} \rightarrow \mathrm{K}\pi(\mathrm{K})$ was derived. The larger combinatorial background required tighter selection criteria. To suppress background from light quarks events, a secondary vertex significantly separated from the beamspot was required by selecting events with $d/\sigma_d > 2.0$, with d being the decay distance. In addition the obtained B mass resolution, which is given by the charged tracking only, is better. Still a very high efficiency, ~ 12.5, was obtained.

Figure 13 shows the invariant mass spectra for the two different mass hypothesis, Kπ and KK. Preliminary results are summarized in table 2.

References

[1] R. Ammar et al. (CLEO), *Evidence for penguins: First Observation of* $\mathrm{B} \rightarrow \mathrm{K}^*(892)\gamma$, CNLS 93-1212.

[2] Albrecht et al. (ARGUS), *Phys. Lett.* B229 (1989) 304.

[3] Avery et al. (CLEO) , *Phys. Lett/* B223 (1989) 470.

[4] P.D. Acton et al. (OPAL), CERN PPE/92-116.
A. De Angelis, F. Scuri, L. Vitale, *Inclusive Production of the ϕ(1020) in the Hadronic Decays of the* Z^0, DELPHI 93-24 PHYS 270.

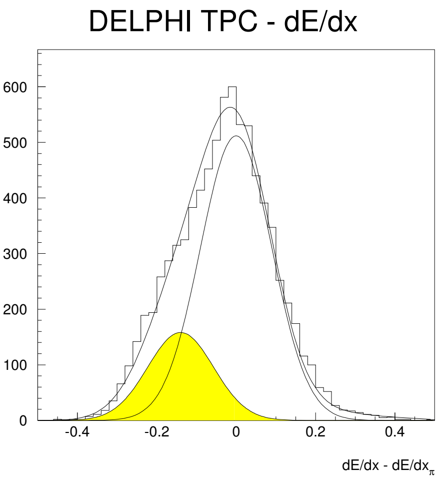

Figure 1: Particle Identification using the specific ionization in the DELPHI TPC (dE/dx). The deviation of the measured ionization of tracks from the specific ionization of pions in hadronic events is shown. The fraction of tracks from Kaons can be determined by a combined fit of the expected shapes of the distribution for different particles.

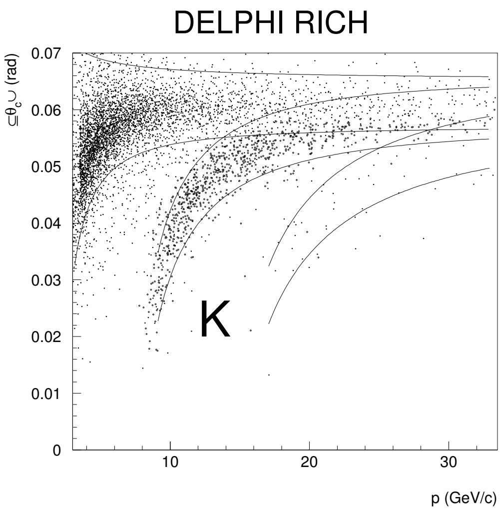

Figure 2: Particle Identification using the DELPHI BRICH. The average Cherenkov angle $< \theta_C >$ is shown *vs* the momentum of the particle. A clear Kaon band is visible.

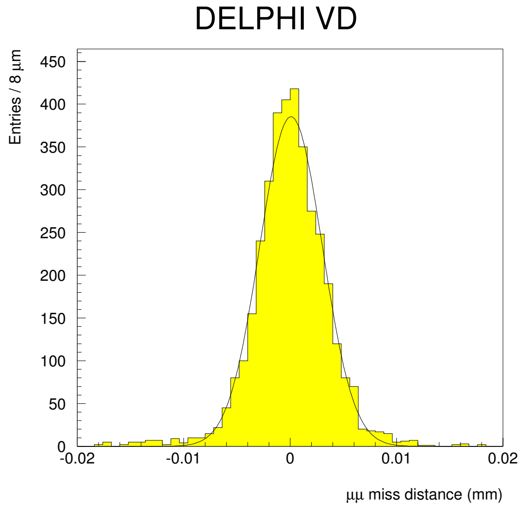

Figure 3: The distance between tracks from the decay $Z^0 \to \mu^+\mu^-$, the so-called 'dimuon miss distance', is used to measure the extrapolation resolution $\sigma_{\rm Extr}$ for high momentum tracks given by the DELPHI VD. The observed width is $\sqrt{2} \times \sigma_{\rm Extr}$.

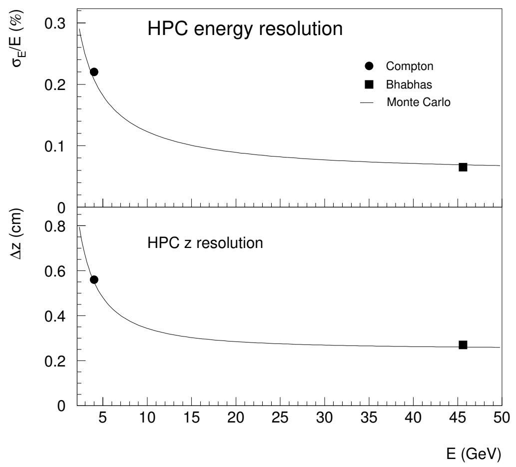

Figure 4: Energy resolution of the DELPHI HPC as a function of the particle energy.

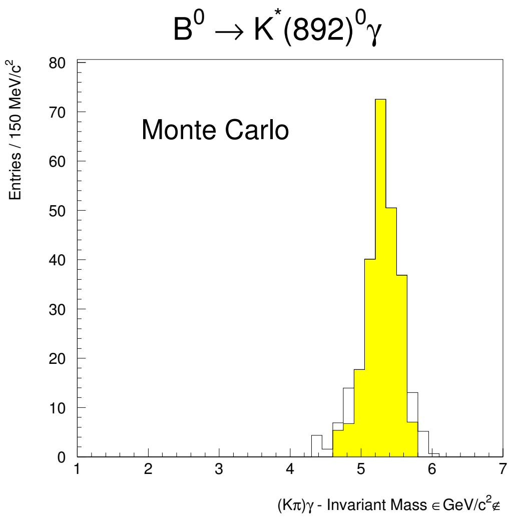

Figure 5: Reconstructed invariant mass of simulated decays $B^0 \rightarrow K^*(892)^0\gamma$. The shaded area indicates the events accepted by the selection criteria.

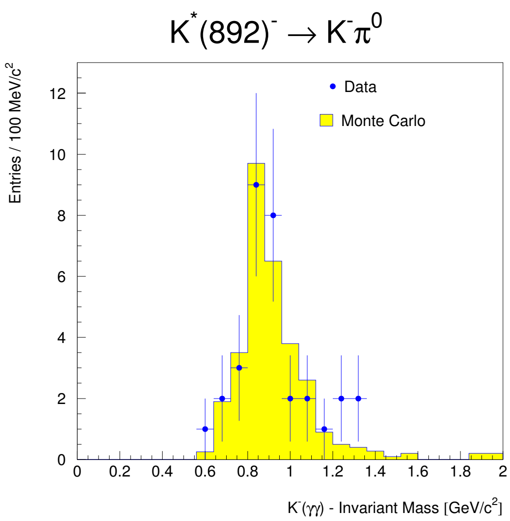

Figure 6: Invariant mass distribution of the decay $\mathrm{K}^*(892)^- \rightarrow \mathrm{K}^-\pi^0$ in of $\mathrm{Z}^0 \rightarrow \tau^+\tau^-$ events.

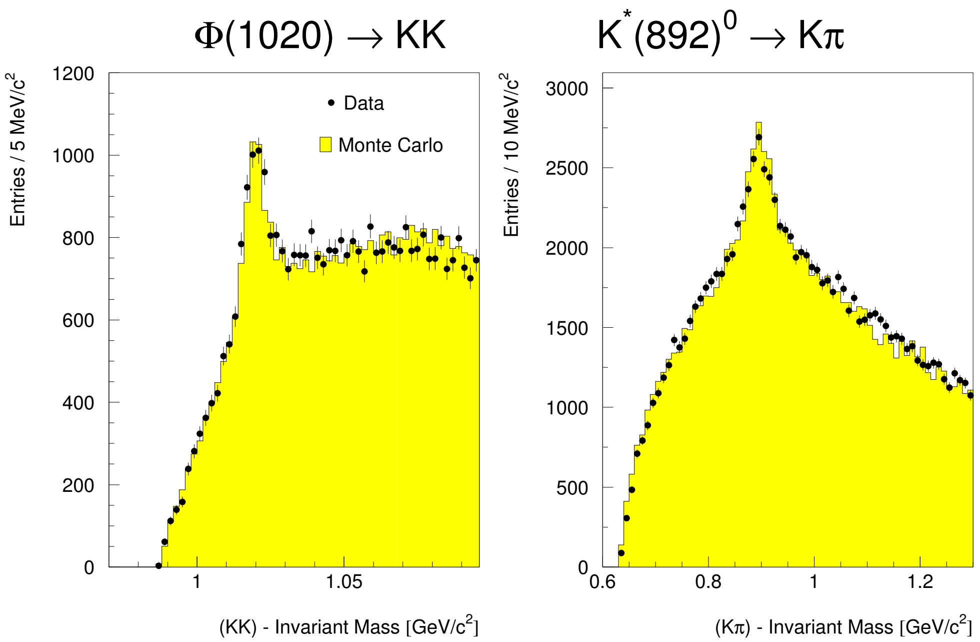

Figure 7: Invariant mass spectra of selected Kπ and KK particles. After reweighting the Monte Carlo events according to the measured particle identification efficiencies and misidentification rates a very good agreement has been reached. The ϕ production rate in the simulation, based on JETSET 7.3 PS, has been reweighted according to the recent measurement of the cross-section by DELPHI [4].

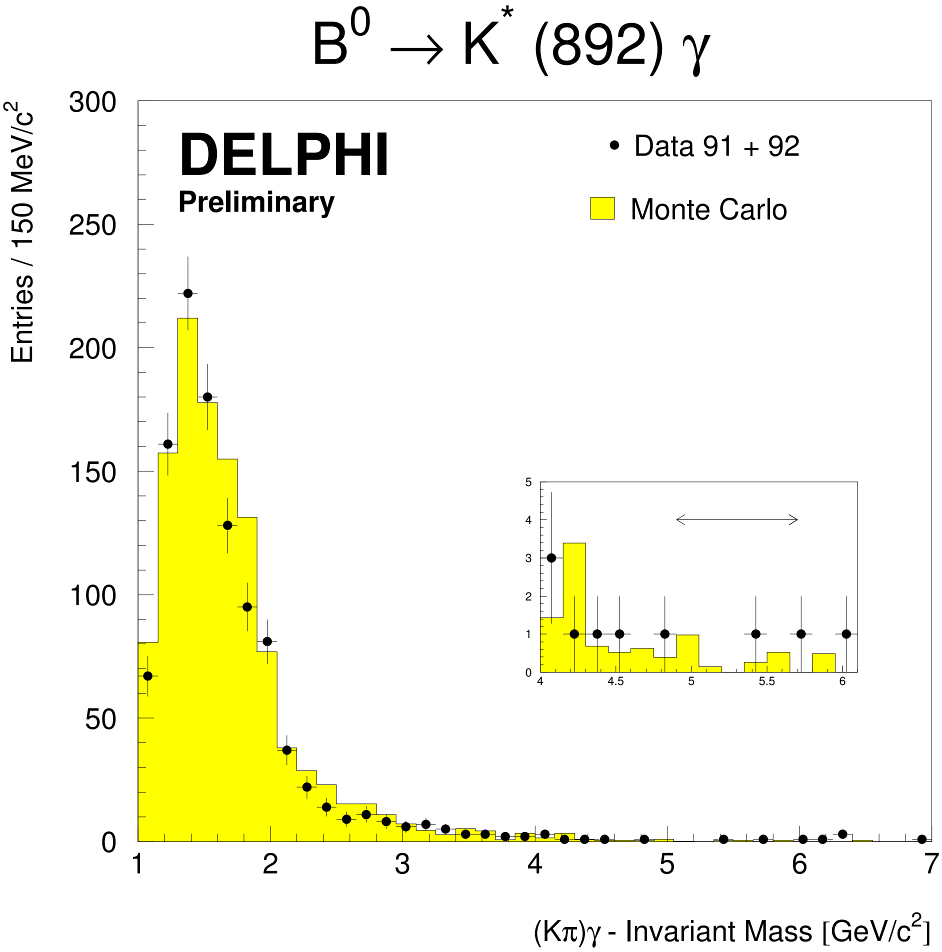

Figure 8: Invariant mass distributions for data and for Monte Carlo simulation of $K^*(892)^0\gamma$ combinations are shown. The arrow is indicating the interval of interest for B^0 decays.

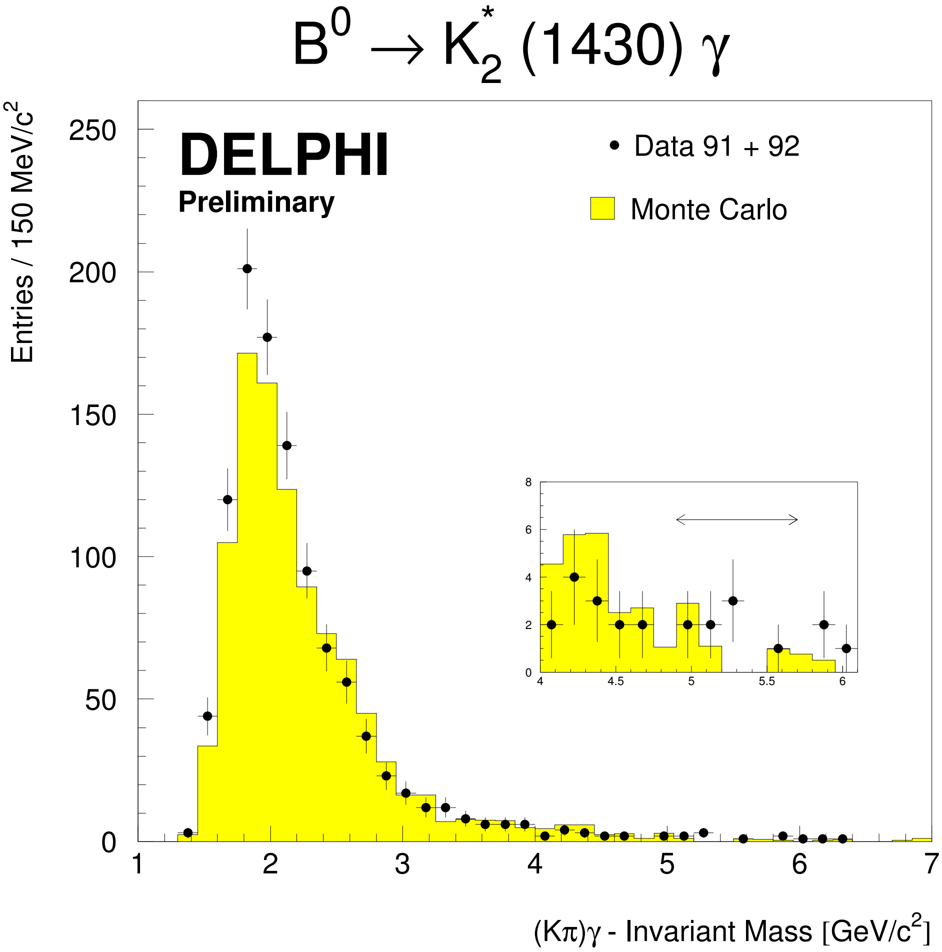

Figure 9: Invariant mass distributions for data and for Monte Carlo simulation of $K_2^*(1430)^0\gamma$ combinations are shown. The arrow is indicating the interval of interest for B^0 decays.

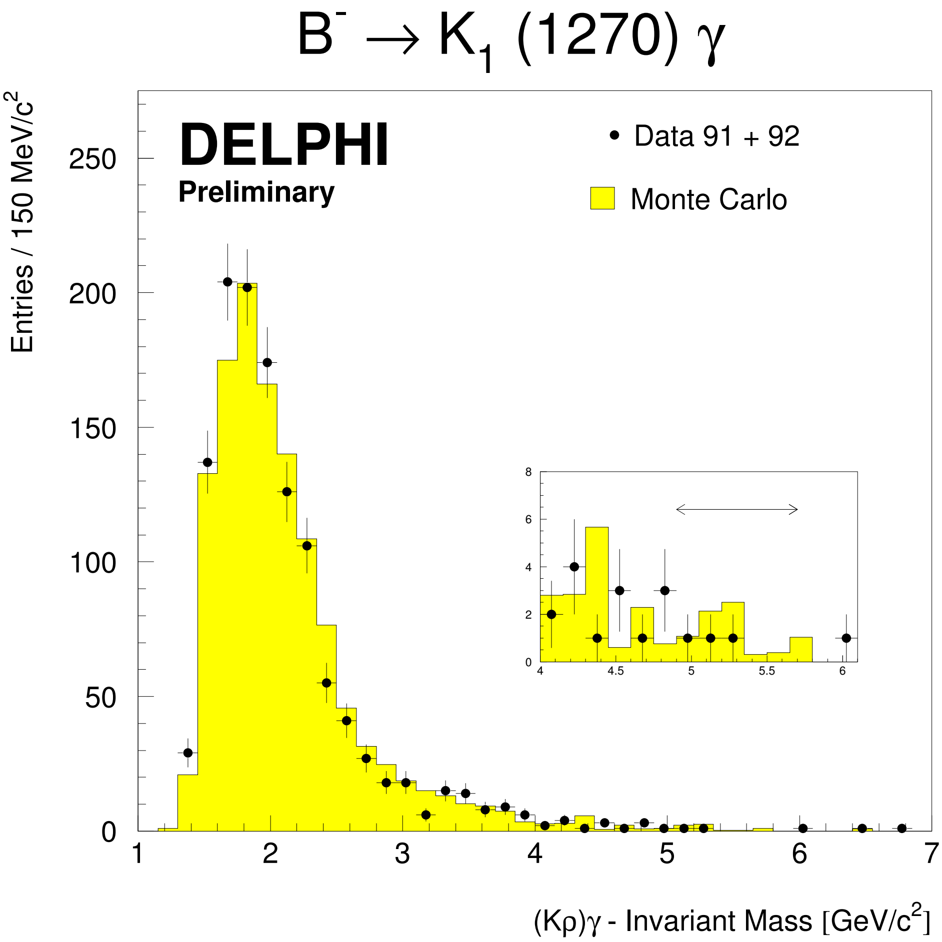

Figure 10: Invariant mass distributions for data and for Monte Carlo simulation of $K_1(1270)^0\gamma$ combinations are shown. The arrow is indicating the interval of interest for B^- decays.

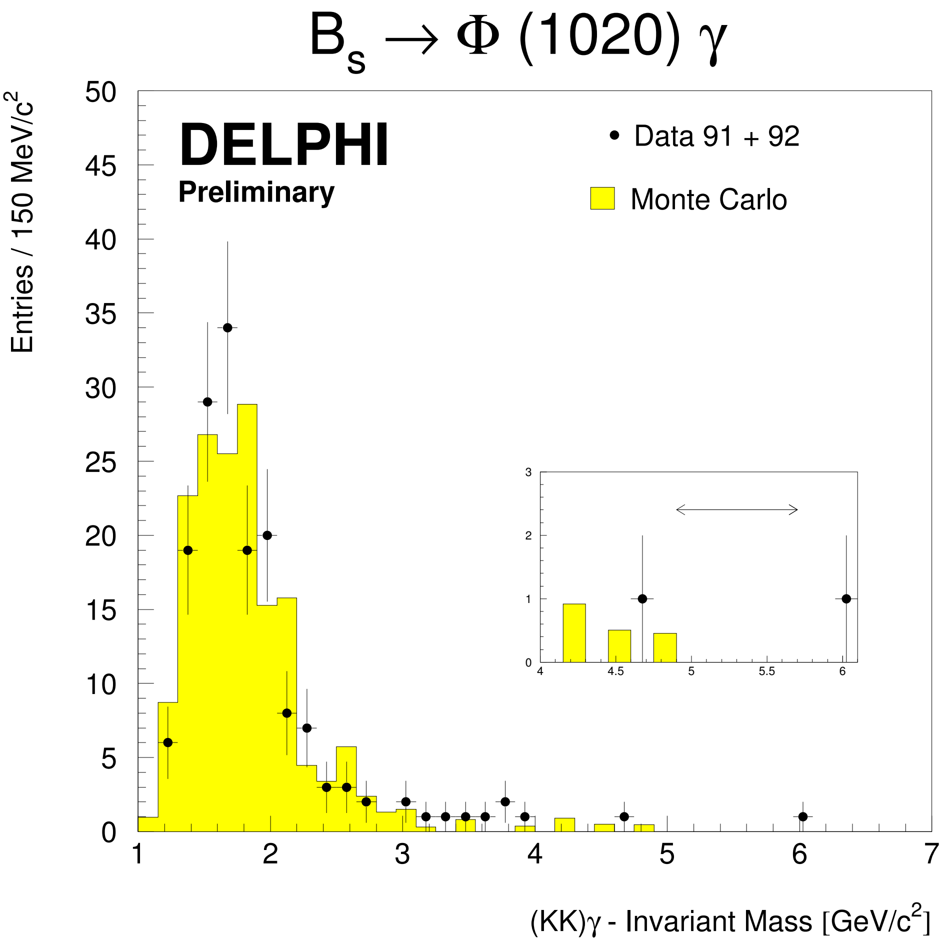

Figure 11: Invariant mass distributions for data and for Monte Carlo simulation of $\phi(1020)^0\gamma$ combinations are shown. The arrow is indicating the interval of interest for B_s decays.

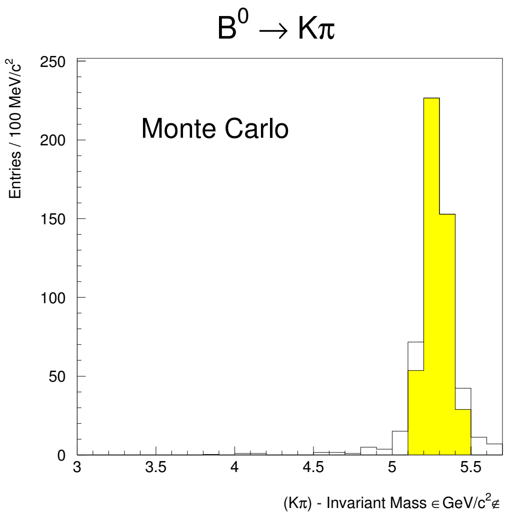

Figure 12: Reconstructed mass of simulated decays $B^0 \to \mathrm{K}\pi$. The shaded area indicates the events accepted by the selection criteria.

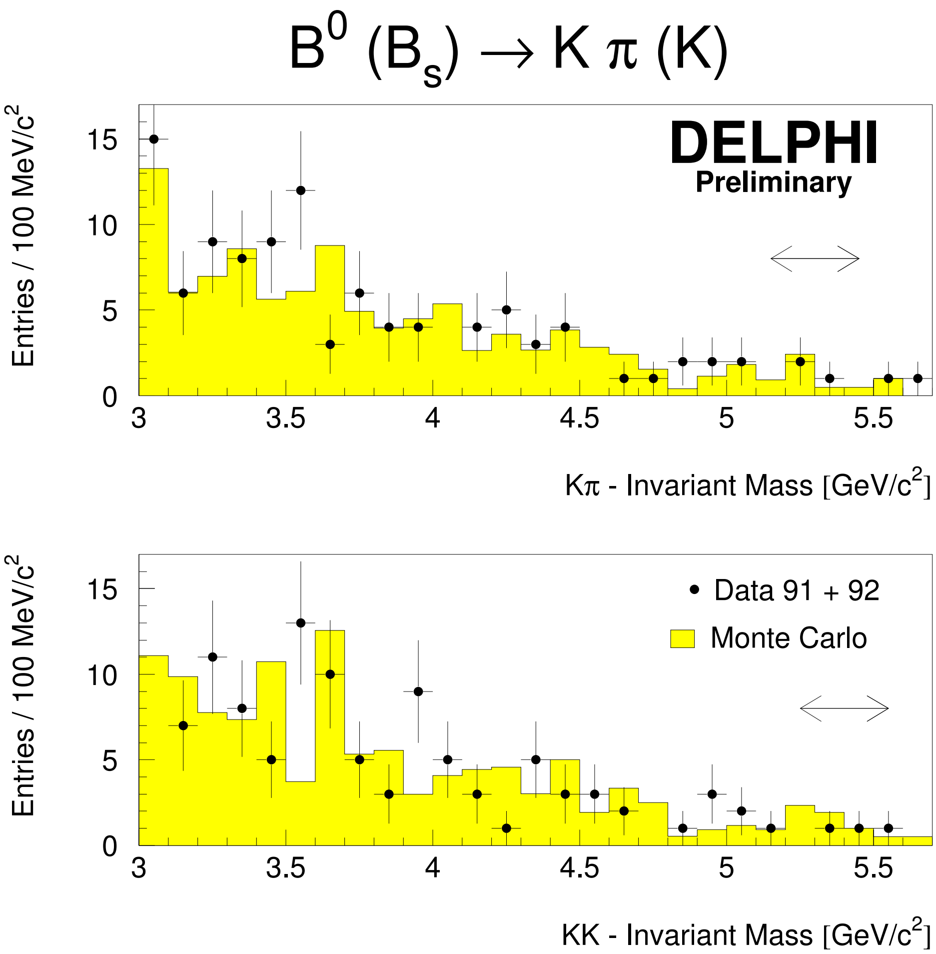

Figure 13: Invariant Mass distribution for data and Monte Carlo simulation of $K\pi$ and KK combinations is shown. The arrow is indicating the interval of interest for decays of the B_d^0 and B_s^0.